Studia Geotechnica et Mechanica, Vol. XXIX, No. 3–4, 2007

ASYMPTOTIC BEHAVIOUR OF SAND IN PLANE-STRAIN COMPRESSION TESTS

DARIUSZ WANATOWSKI

Lecturer, Nottingham Centre for Geomechanics, School of Civil Engineering,
The University of Nottingham, University Park, Nottingham NG7 2RD, United Kingdom.
E-mail: dariusz.wanatowski@nottingham.ac.uk
Visiting Fellow, School of Aerospace, Civil and Mechanical Engineering, University of New South Wales at Australian Defence Force Academy, Canberra, ACT 2600, Australia.

Abstract: Experimental data are presented, which allows the asymptotic behaviour of sand under plane-strain conditions to be studied. K_0 consolidated plane-strain tests were conducted using a new plane-strain apparatus under strain path-controlled conditions. The stress–strain behaviour of sand in very loose and medium dense states under plane-strain conditions was characterized. The results show that the stress–strain behaviour of sand under plane-strain conditions is strain path-dependent. When the strain increment ratio imposed on specimens $(d\varepsilon_v/d\varepsilon_1)_i$ is higher (i.e., more positive) than a threshold value, strain hardening behaviour will prevail. On the other hand, when the $(d\varepsilon_v/d\varepsilon_1)_i$ is lower (i.e., more negative) than a threshold value, strain softening will occur. The threshold strain increment ratio is defined as $(d\varepsilon_v/d\varepsilon_1)_f$, that is the strain increment ratio at failure as measured in a drained test. It is also observed that the asymptotic behaviour of sand cannot be predicted by the Cam clay models or the Rowe's stress–dilatancy equation. This is consistent with the observations made by other researchers under axisymmetric conditions.

Streszczenie: Przedstawione dane doświadczalne umożliwiają badanie asymptotycznego zachowania się piasku w warunkach płaskiego stanu odkształcenia. Badania przeprowadzono w warunkach kontrolowanego płaskiego stanu odkształcenia z konsolidacją w jednoosiowym stanie odkształcenia, korzystając z nowo zaprojektowanego aparatu dwuosiowego ściskania. Scharakteryzowano zależności pomiędzy naprężeniami i odkształceniami dla piasku w stanie luźnym i średnio zagęszczonym. Otrzymane wyniki świadczą, że zależności między naprężeniami i odkształceniami próbek piasku w warunkach płaskiego stanu odkształcenia zależą od kontrolowanej ścieżki naprężeń. Jeśli współczynnik przyrostu odkształcania $(d\varepsilon_v/d\varepsilon_1)$, któremu poddano próbki, przekracza wartość graniczną (tzn. jest bardziej dodatni), to próbki ulegają wzmocnieniu. Jeśli zaś wartość tego współczynnika jest niższa od wartości granicznej (tzn. jest bardziej ujemna), to próbki ulegają osłabieniu. Graniczny współczynnik przyrostu odkształcenia jest zdefiniowany jako $(d\varepsilon_v/d\varepsilon_1)$, tj. współczynnik przyrostu odkształcenia zmierzony w momencie ścięcia próbki w badaniu wytrzymałościowym metodą ścinania powolnego z odpływem wody. Na podstawie przeprowadzonych badań stwierdzono również, że asymptotycznego zachowania się piasku nie można przewidzieć ani opierając się na modelach gliny Cam, ani na równaniu Rowe'a opisującym zależność naprężenia od dylatacji. Jest to zgodne z obserwacjami poczynionymi przez innych badaczy w warunkach symetrii osiowej.

Резюме: Представленные экспериментальные данные дают возможность исследования асимптотического поведения песка в условиях плоского состояния деформации. Исследования были проведены в условиях контролируемого плоского состояния деформации, с использованием новозапроектированного аппарата двухосного сжатия. Схарактеризованы зависимости между напряжениями и деформациями для песка в рассыпчатом и в свободном среднем компактном состояниях. Полученные результаты свидетельствуют о том, что зависимости между напряжениями и деформациями проб песка в условиях плоского состояния деформации зависят от

контролируемой дороги напряжений. Если коэффициент прироста деформации ($d\varepsilon_v/d\varepsilon_1$), которой были родвержены пробы, превышает предельное значение (т.е. является более положительным), то пробы подвергаются ослаблению. Предельный коэффициент прироста деформации определён как ($d\varepsilon_v/d\varepsilon_1$), т.е. коэффициент прироста деформации, измеренный в момент срезывания образца в прочностном исследовании методом медленного срезывания с отливанием воды. На основе проведенных исследований было также установлено, что невозможно предвидение асимптотического поведения песка ни базируя на моделях глины Кам, ни на уравнении Роуа, описывающем зависимость напряжения от дилатации. Это согласно с наблюдениями, выполненными другими исследователями в условиях осевой симметрии.

LIST OF SYMBOLS

D – dilatancy factor $D = 1 - d\varepsilon_v/d\varepsilon_1$,
$-d\varepsilon_v/d\varepsilon_1$ – dilatancy ratio,
$d\varepsilon_v/d\varepsilon_1$ – strain increment ratio,
e – void ratio,
p' – mean effective stress, $p' = \frac{1}{3}(\sigma_1' + \sigma_2' + \sigma_3')$,
q – deviatoric stress, $q = \frac{1}{\sqrt{2}}[(\sigma_1 - \sigma_2)^2 + (\sigma_2 - \sigma_3)^2 + (\sigma_3 - \sigma_1)^2]^{1/2}$,
ε_1 – axial strain,
ε_v – volumetric strain,
ϕ' – effective friction angle of soil,
η – effective stress ratio, $\eta = q/p'$,
θ – angle of the shear band orientation.

SUBSCRIPTS

asy – asymptotic,
c – consolidated,
cs – critical state,
f – failure,
i – imposed.

1. INTRODUCTION

When the stress–strain behaviour of soil is studied experimentally, laboratory tests can be controlled using either stress path or strain path method. The stress path method was originally described by LAMBE [18] and used to predict the settlement of foundations. Since then, this method has become very popular for both practising engineers and researchers. A typical example of a stress path test is the conventional drained triaxial compression test, in which the cell pressure is held constant and the axial load is increased. This corresponds to a controlled stress path test with a $d\sigma_3' = 0$.

The strain path method was originally proposed by CHU and LO [5] to study strain softening behaviour of sand. In this method, a strain path can be specified by the strain increment ratio $d\varepsilon_v/d\varepsilon_1$. By using digital pressure volume controllers [24] linked to a computer, $d\varepsilon_v/d\varepsilon_1$ can be precisely controlled and all possible drainage conditions can be simulated [5]. When $d\varepsilon_v/d\varepsilon_1 > 0$, the soil specimen will compress and water will flow out of the sample with axial deformation. On the other hand, when $d\varepsilon_v/d\varepsilon_1 < 0$, the sample will dilate and water will flow into the specimen. An undrained test is only a special case of general drainage conditions with $d\varepsilon_v/d\varepsilon_1 = 0$.

It has been long recognised that the stress–strain behaviour of soils is path-dependent. The stress–strain response of soil can be entirely different when a specimen is sheared under different paths [15], [22]. Although both stress and strain paths can affect constitutive behaviour of soils, the strain path testing method is less popular among geotechnical engineers and researchers. Consequently, the studies on the stress–strain behaviour of soils under various strain paths are very limited.

One of the first experimental studies using strain path method was conducted by CHU et al. [6], [7] to study strain softening and instability behaviours of sand. CHU et al. [6] reported that the occurrence of strain softening depends on both the increment ratio of the strain ($d\varepsilon_v/d\varepsilon_1$) imposed on the specimen and the initial mean effective stress p'_0. Furthermore, CHU et al. [7] proposed a comparison of $d\varepsilon_v/d\varepsilon_1$ imposed on the specimen with the maximum dilation rate at failure, measured by $d\sigma'_3 = 0$ test, as the criterion for instability to occur. It has been observed that instability can occur even for a dense sand specimen if the strain increment ratio imposed is lower than that at failure measured in the $d\sigma'_3 = 0$ test. Similar experiments have been conducted by other researchers [19], [35] who have also observed that pre-failure strain softening and pre-failure instability can occur for dense sand when tested in a triaxial cell along a strain path with $d\varepsilon_v/d\varepsilon_1 < 0$. These observations have also been extended to multi-axial conditions [9].

The strain path testing method [5] has also been used to study an asymptotic behaviour of a granular soil [8]. The term *asymptotic behaviour* was first introduced by GUDEHUS et al. [14] to describe a response of soil along proportional stress/strain paths. The results presented in [14] show that when a soil is sheared along some $\sigma'_1/\sigma'_3 = \text{const}$ paths, the strain approach $d\varepsilon_v/d\varepsilon_1 = \text{const}$ state instead of a critical state. Experimental data obtained for Sydney sand using triaxial and multi-axial cells [8], [9] indicated further that when a granular soil is sheared along $d\varepsilon_v/d\varepsilon_1 = \text{const}$ paths, the stress ratio will approach a straight line, called *the constant stress ratio line* (CSRL). Therefore, the asymptotic state may be defined as the state where a soil element deforms under a constant stress mobilized level and a constant dilatancy ratio state, that is when $q/p' = \text{const}$ and $d\varepsilon_v/d\varepsilon_1 = \text{const}$. Similar observations have also been made for clay using a biaxial cell [34].

It has been suggested that a limited number of strain path tests reported in the literature might be a consequence of the complexity of the existing strain path testing

methods [31]. Therefore, a simplified method for strain path testing using a double-cell triaxial apparatus has been proposed [31]. In this method, the size of the top cap before a test was adjusted to apply several constant strain paths. The advantage of this method is that both saturated and unsaturated soil specimens can be tested. However, in this method only limited range of strain paths can be imposed due to the confined space of the triaxial cell to allow for the adjustment of the top cap sizes. As a result this method has not been widely accepted.

Strain softening or instability of sand has often been investigated experimentally under undrained conditions [4], [16], [17], [21], [33], [37]. However, in most practical problems, a soil element may experience both volume change and pore water pressure change simultaneously [36], [38]. Furthermore, failure mechanisms related to a redistribution of void ratio within a globally undrained sand layer and the spreading of excess pore pressure with global volume changes have also been defined by the National Research Council [26], as shown in figure 1. ADALIER and ELGAMAL [1] also reported a pore water pressure increase and a potential strength loss in the dense granular soil due to the migration of pore water into the dense zone from the adjacent loose zone.

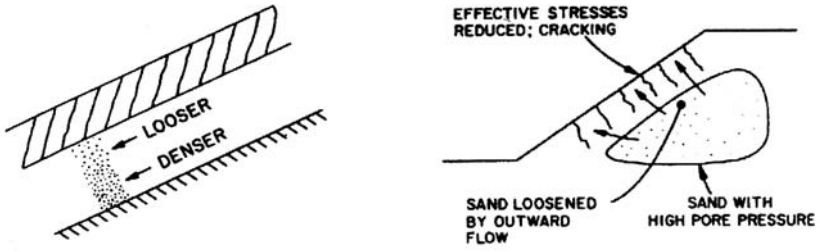

a) b)

Fig. 1. Failure mechanisms defined by NRC: a) mechanism B: situation for void redistribution within a global sand layer, b) mechanism C: situation for failure by the spreading of excess pore pressure with global volume changes [26]

A number of tests on loose and dense granular materials under strain path-controlled conditions have been conducted by CHU and LEONG [10]. It was observed that the liquefied soil in an ordinary undrained test reaches eventually a steady state, but the unstable soil in a strain path test collapses with a pore water pressure increase to the cell pressure level. A similar study was also carried out by VAID and ELIADORANI [35]. The authors reported that the small expansive volumetric strains resulting from the strain path-controlled condition could render an initial state that would have been stable under undrained deformation into an unstable state. Therefore, an undrained condition, commonly assumed as the most conservative, may not be the most dangerous situation. This unstable behaviour of potentially non-liquefiable soils emphasizes the importance of the strain path testing method because such a behaviour can only be simulated in the laboratory by controlling the strain increment ratio $d\varepsilon_v/d\varepsilon_1$, as described earlier. It should

also be noted that different terms are used in the literature for the condition, in which the dilation of the sand is controlled. CHU et al. [6], [7] proposed the term *non-undrained condition*, whereas VAID and ELIADORANI [35] suggested the term *partially drained condition*. However, to avoid any misconception about drainage conditions, the term *strain path-controlled condition* will be used in this paper.

It should be pointed out that almost all above mentioned experimental studies on the influence of strain path on the stress–strain behaviour of granular soils have been carried out in triaxial cells. To the author's knowledge, no study on the stress–strain behaviour of sand using strain path testing has been conducted under plane-strain conditions, which cover most practical situations in geotechnical engineering.

The objective of this paper is to study the stress–strain behaviour of sand in strain path testing under plane-strain conditions. The results of the strain path ($d\varepsilon_v/d\varepsilon_1$ = constant) tests conducted on very loose and medium dense sand are presented. The asymptotic behaviour of sand under plane-strain conditions is discussed.

2. TEST ARRANGEMENT

The plane-strain test arrangement used in this study is shown in figure 2. A prismatic soil specimen of 120 mm in height and 60 mm × 60 mm in cross-section was tested. Two 35-mm thick stainless steel vertical platens were fixed in position by two pairs of horizontal tie rods to impose a plane-strain condition. The lateral stress in this direction (σ_2) was measured by four submersible total pressure transducers. As shown in figure 2, two transducers were used for each platen, so that the lateral pressures at both the top and the bottom positions of the specimen could be measured and any non-uniform stress distribution could be detected. The total lateral pressure was evaluated as an average value obtained from the four individual transducers. All rigid platens were properly enlarged and lubricated using the free-end technique [30] to reduce the boundary friction and to delay the occurrence of non-homogeneous deformations. For the top and base free-ends, latex disks were used, whereas for the vertical free-ends Teflon sheets were used. A pair of miniature submersible linear variable differential transformers (LVDTs) were used to measure the vertical displacement. An external LVDT was also used to measure the axial strain when the internal LVDTs ran out of travel. As shown in figure 2, a digital hydraulic force actuator was mounted at the bottom of a loading frame to apply axial load. The actuator was controlled by a computer via a digital load/displacement control box. The cell pressure was applied through a digital pressure/volume controller (DPVC). Second DPVC was used to control the back pressure from the bottom of the specimen while measuring the volumetric change at the same time. A pore pressure transducer was used to record the pore water pressure at the top of the specimen. For details of the plane-strain apparatus, see [39], [40].

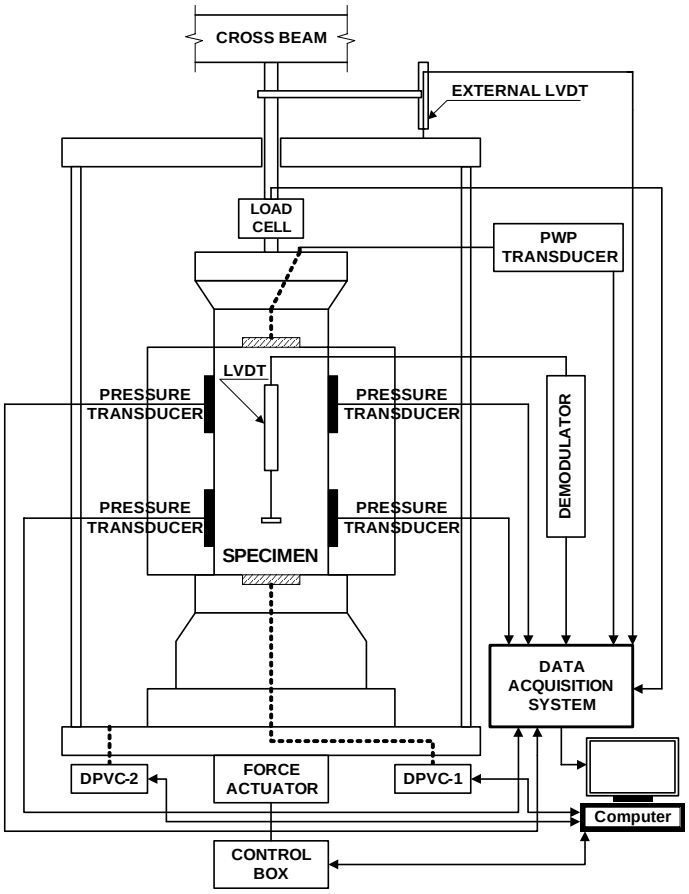

Fig. 2. The plane-strain test arrangement

3. MATERIALS AND METHODOLOGY

All tests presented in this paper were conducted on Changi sand, a marine dredged silica sand used for the Changi land reclamation project in Singapore. The basic properties of the sand are given in table 1. For a detailed description of the physical and mechanical properties of the sand, see [20]. Laboratory reconstituted specimens prepared either by the water sedimentation (WS) or the moist tamping (MT) method were used. A liquid rubber technique [21] was adopted to reduce the effect of membrane penetration. In this method, a thin layer of liquid rubber was coated onto the inner side of the membrane before the placement of sand. A back pressure of 400 kPa was applied in all the tests to ensure the complete saturation of the specimens.

T a b l e 1

Basic properties of the tested sand

Specific gravity	Mean size [mm]	Coefficient of uniformity	Coefficient of curvature	Max. void ratio	Min. void ratio	Fines content [%]	Shell content [%]
2.60	0.30	2.0	0.8	0.916	0.533	0.4	12–14

4. TESTING PROGRAM

The behaviour of sand under plane-strain conditions in the present study was investigated in a wide range of linear strain paths. The strain paths used in the experiments in the form of strain increment ratios ($d\varepsilon_v/d\varepsilon_1$) are schematically presented in figure 3. All specimens were K_0 consolidated from an initial isotropic stress state of 20 kPa to the stress state required. The K_0 condition was imposed by regulating the volume change of the specimen in accordance with the axial strain to maintain $d\varepsilon_v/d\varepsilon_1 = 1$ [23]. It should be pointed out that the back pressure level at the end of K_0 consolidation was taken as the datum and the decrease in pore water pressure was noted as negative. After K_0 consolidation the specimens were sheared along either a dilative ($d\varepsilon_v/d\varepsilon_1 < 0$) or compressive ($d\varepsilon_v/d\varepsilon_1 > 0$) strain path. All the tests were conducted in deformation-controlled mode at a rate of 0.05 mm/min. A summary of all the plane-strain tests conducted is given in table 2.

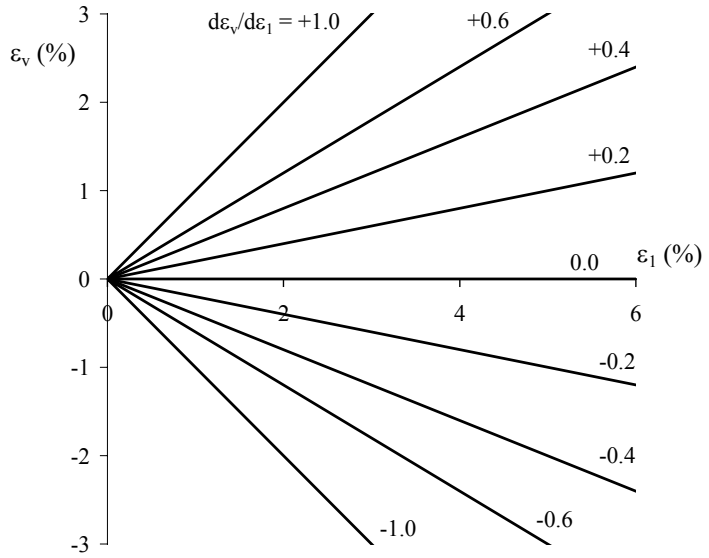

Fig. 3. A range of strain paths imposed in plane-strain tests

Table 2

Summary of plane-strain tests conducted

Test No.	Preparation method	e_c	Dr_c (%)	Density state*	p'_c (kPa)	q_c (kPa)	$(d\varepsilon_v/d\varepsilon_1)_i$
SP02	WS	0.684	61	m. dense	201.0	211.1	–0.2
SP04	MT	0.897	5	v. loose	195.9	169.8	–0.2
SP05	WS	0.677	62	m. dense	198.2	220.3	–0.4
SP08	MT	0.890	7	v. loose	200.6	172.4	–0.4
SP26	WS	0.731	48	m. loose	404.5	421.7	–0.4
SP09	WS	0.679	62	m. dense	200.0	222.4	–0.6
SP12	MT	0.887	8	v. loose	199.8	169.0	–0.6
SP13	WS	0.682	61	m. dense	201.5	210.7	–1.0
SP14	WS	0.694	58	m. dense	202.9	218.1	+0.2
SP16	MT	0.888	7	v. loose	197.8	174.3	+0.2
SP17	WS	0.682	61	m. dense	200.5	227.3	+0.4
SP19	MT	0.878	10	v. loose	199.6	174.3	+0.4
SP20	WS	0.681	61	m. dense	206.2	226.4	+0.6
SP22	MT	0.903	3	v. loose	197.5	171.9	+0.6
SP23	WS	0.686	60	m. dense	202.8	226.6	+1.0
U02	WS	0.695	58	m. dense	201.9	218.8	0.0
U08	MT	0.902	4	v. loose	198.4	168.4	0.0

Note: *Density description of SKEMPTON [32] is adopted: very loose (D_r < 15%); loose (D_r = 15–35%); medium loose (D_r = 35–50%); medium dense (D_r = 50–65%); dense (D_r > 65%).

5. RESULTS

Drained tests. The drained behaviour of Changi sand has been reported elsewhere [40], [41]. Therefore, only a brief summary is presented in this section as a basis for further analysis. Stress–strain curves obtained from drained plane-strain tests conducted on medium dense, medium loose and very loose Changi sand are plotted in figures 4a to 4c, respectively. All the tests were K_0-consolidated to p'_c = 100, 200 and 300 kPa and then sheared under drained conditions with σ'_3 maintained constant. It can be seen from figures 4a and 4b that during drained shearing of medium dense and medium loose specimens, the deviatoric stress firstly reached a peak, and then reduced gradually to a constant ultimate value. It should be pointed out that the peak deviatoric stress in these tests was accompanied by shear band formation. The $q-\varepsilon_1$ curves of drained tests conducted on very loose sand are presented in figure 4c. It is observed that the deviatoric stress approached a constant value at the end of each test. As reported by WANATOWSKI and CHU [40] the volumetric strain in these tests also approached a constant value. Furthermore, shear bands have not been detected either. Therefore, it can be concluded that the critical state is reached in these tests.

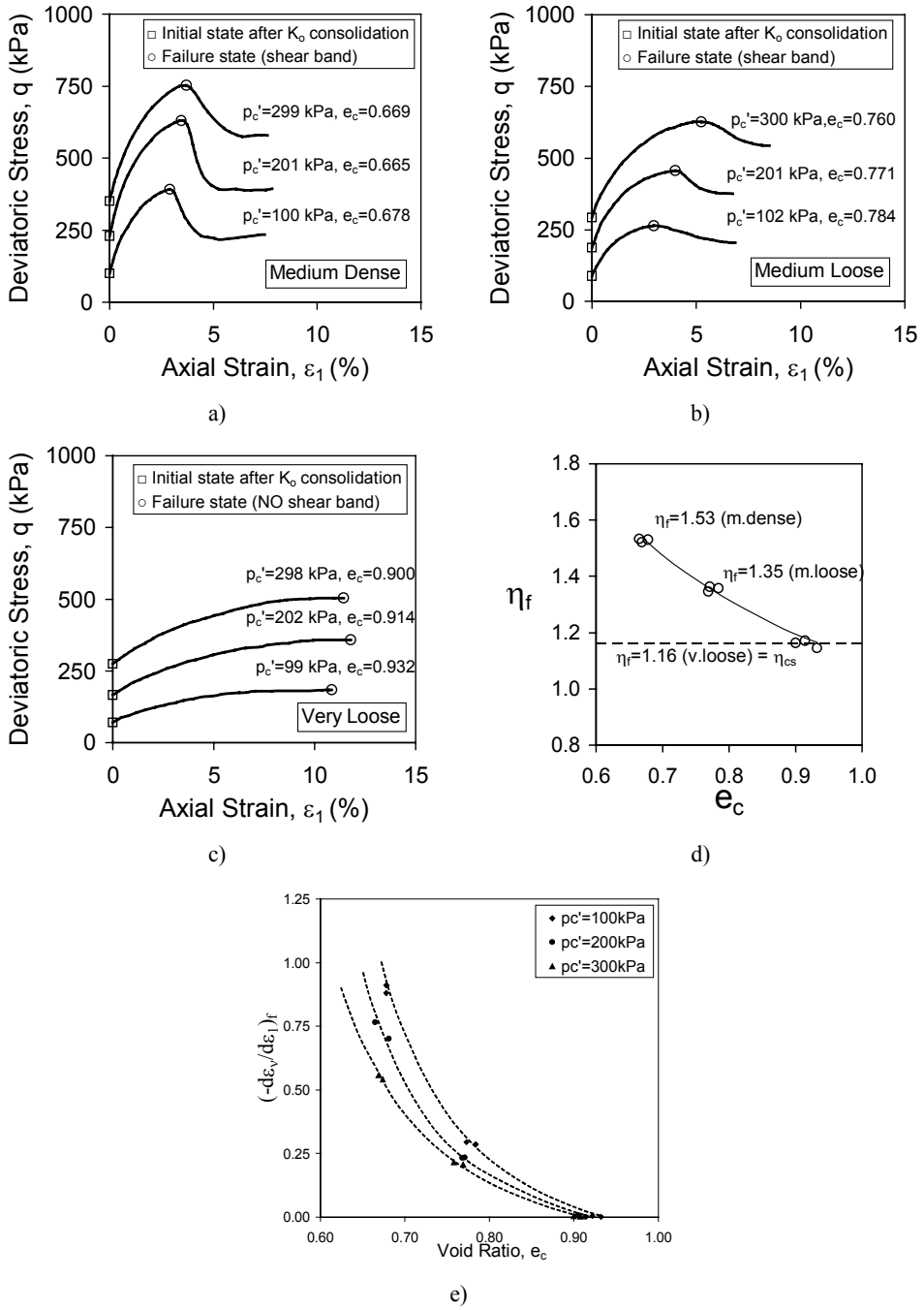

Fig. 4. Drained behaviour of the Changi sand: a) medium dense, b) medium loose, c) very loose, d) summary of failure states, e) relationship between $(-d\varepsilon_v/d\varepsilon_1)_f$ and e_c

A summary of all failure states obtained from the plane-strain tests is shown in figure 4d. Under plane-strain conditions, the slopes of the failure lines (η_f) for very loose, medium loose and medium dense sands are 1.16, 1.35, and 1.53, respectively. These values correspond to the friction angles (ϕ_f) of 36.0°, 43.4°, and 49.7°, respectively. Since the failure line for very loose sand is also the CSL, η_{cs} =1.16 and ϕ_{cs} = 36.0° [40], [41]. A further summary of the failure states is given in figure 4e, where the relationship between maximum dilatancy ratio at failure $(-d\varepsilon_v/d\varepsilon_1)_f$ and void ratio (e_c) is given. It should be stressed that this relationship is affected by p'_c.

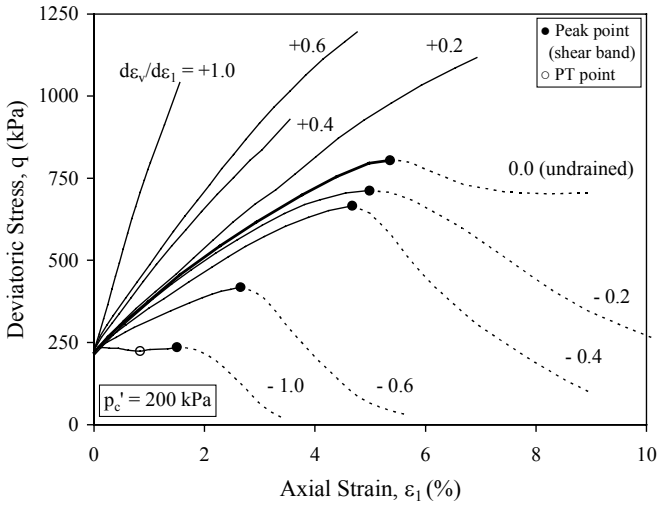

a)

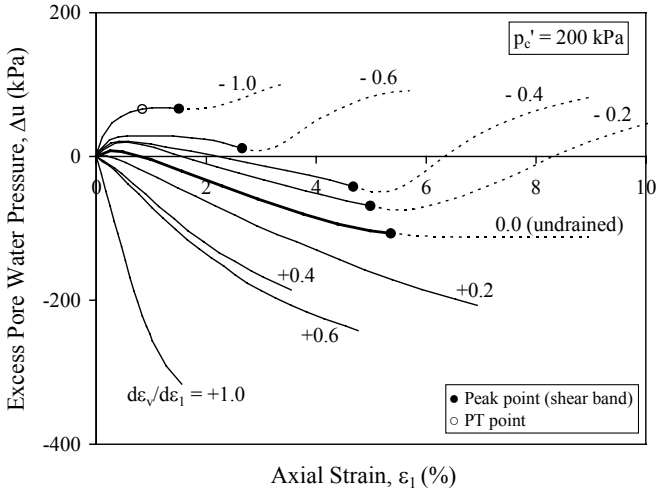

b)

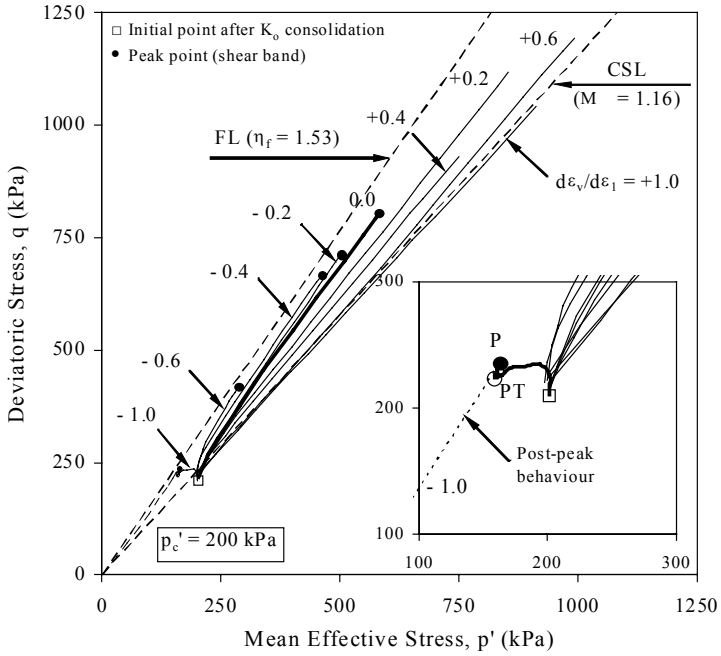

c)

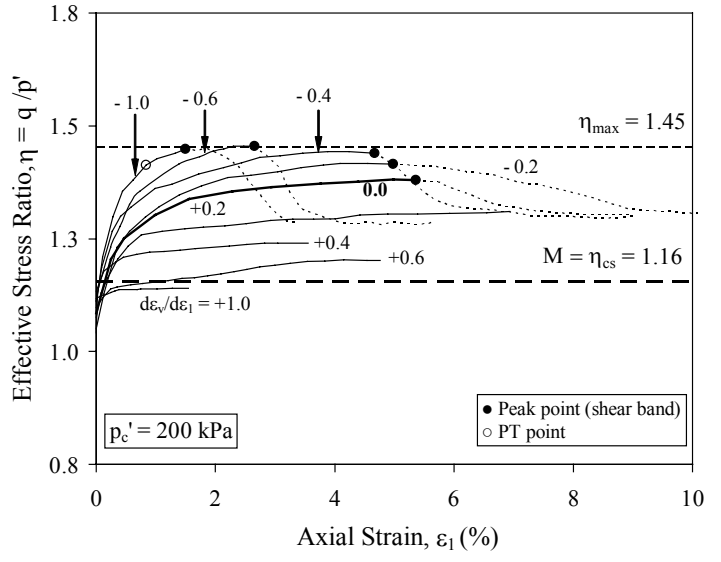

d)

Fig. 5. Strain path-dependent behaviour of medium dense sand:
a) stress–strain curves, b) excess pore water pressure versus axial strain curves,
c) effective stress paths, d) effective stress ratio versus axial strain curves

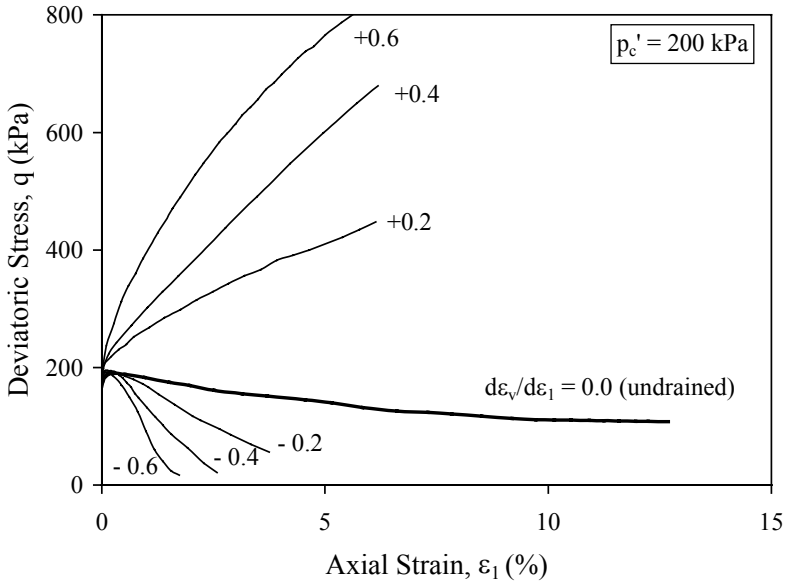
800
600
400
200
0
0
5
10
15
Deviatoric Stress, q (kPa)
Axial Strain, ε1 (%)
+0.6
+0.4
+0.2
dεv/dε1 = 0.0 (undrained)
- 0.2
- 0.4
- 0.6
pc' = 200 kPa

a)

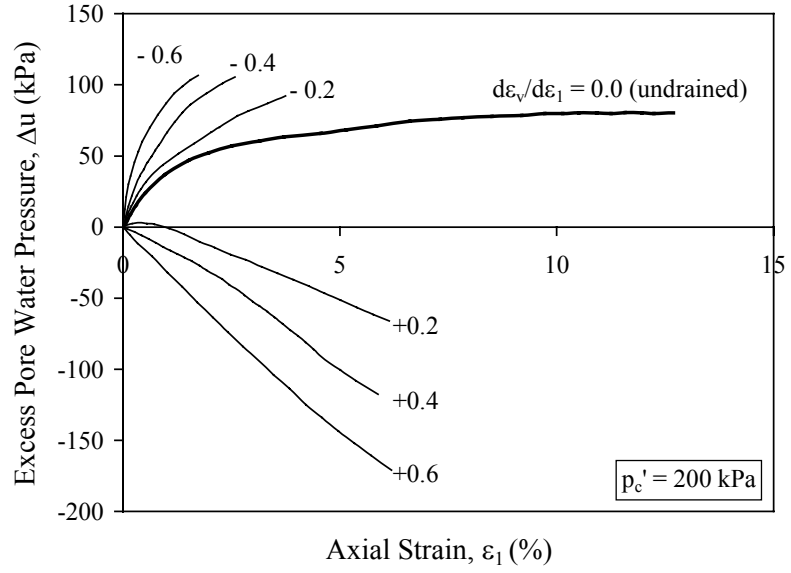
150
100
50
0
-50
-100
-150
-200
0
5
10
15
Excess Pore Water Pressure, Δu (kPa)
Axial Strain, ε1 (%)
- 0.6
- 0.4
- 0.2
dεv/dε1 = 0.0 (undrained)
+0.2
+0.4
+0.6
pc' = 200 kPa

b)

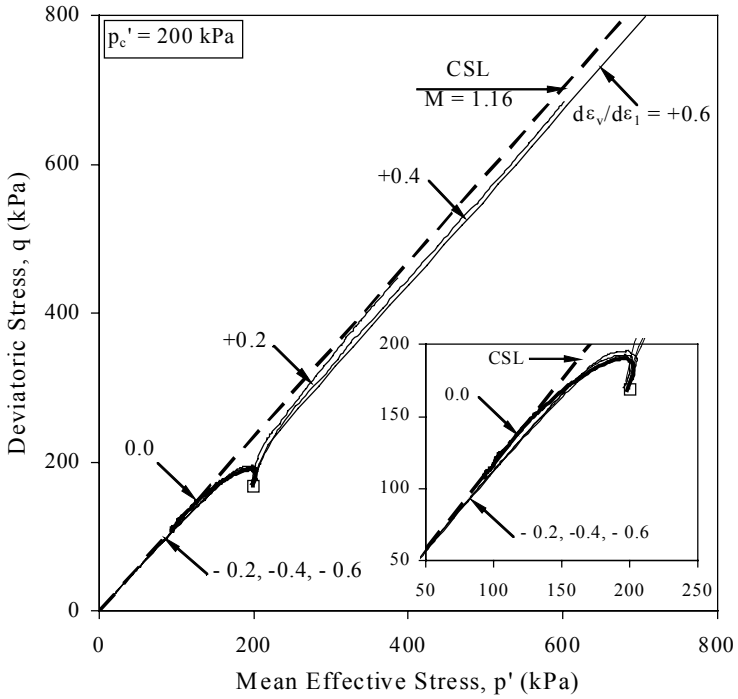

c)

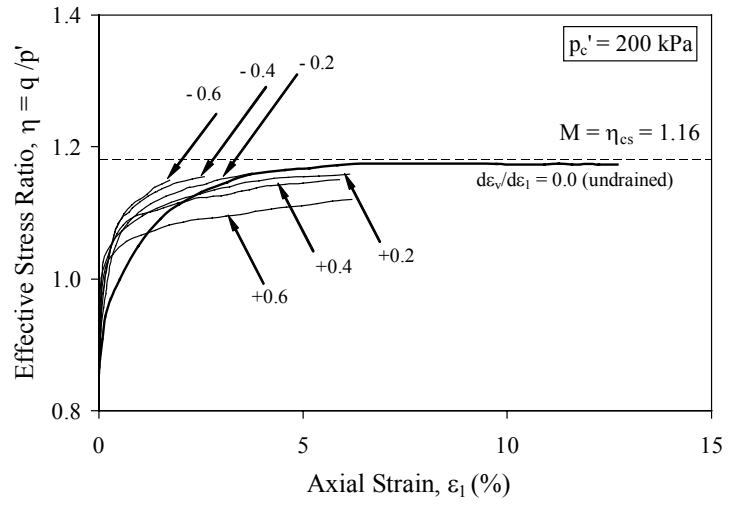

d)

Fig. 6. Strain path-dependent behaviour of very loose sand:
a) stress–strain curves, b) excess pore water pressure versus axial strain curves,
c) effective stress paths, d) effective stress ratio versus axial strain curves

Strain path tests on medium dense sand. The influence of a strain path on the stress–strain behaviour of sand in plane-strain tests is clearly demonstrated in figure 5, where the results of a series of strain path tests conducted on medium dense sand with different strain increment ratios $d\varepsilon_v/d\varepsilon_1$, ranging from +0.1 to –0.1, are presented. The void ratios e_c of specimens after K_0 consolidation were in the range from 0.677 to 0.695, corresponding to relative densities Dr_c = 58–62%. All the specimens were prepared by the WS method. Although all the specimens were in the narrow density range, different types of behaviour, mainly strain hardening and limited strain softening, were observed. The response produced for more compressive (positive) strain paths was strong strain hardening compared to that for more dilative (negative) strain paths. Therefore, for a given axial strain, the higher the strain increment ratio imposed, the stiffer the stress–strain curve obtained, as shown in figure 5a. It can also be seen from figure 5a that stress–strain curves for the strain paths with $d\varepsilon_v/d\varepsilon_1 > 0$ are different from those with $d\varepsilon_v/d\varepsilon_1 \le 0$. For the strain path tests with $d\varepsilon_v/d\varepsilon_1 > 0$, strain hardening behaviour was only observed. As shown in figure 5a, peak state is not reached by any of the $d\varepsilon_v/d\varepsilon_1 > 0$ paths before the termination of the test. There is no visible shear band either. For the strain paths within the range of $-0.6 \le d\varepsilon_v/d\varepsilon_1 \le 0$ the strain hardening behaviour is also observed. However, it is followed by the peak state and the strain softening behaviour in the post-peak region. It should be pointed out that the peak deviatoric stress in these tests coincides with shear band formation. Consequently, banding softening behaviour [9] is observed in $-0.6 \le d\varepsilon_v/d\varepsilon_1 \le 0$ paths. It should also be stressed that the banding softening could have been possibly observed in the $d\varepsilon_v/d\varepsilon_1 > 0$ strain paths if the shearing was further continued. However, the lateral pressures (σ_2) in these tests reached the capacity of the lateral pressure transducers. Thus, the $d\varepsilon_v/d\varepsilon_1 > 0$ strain path tests had to be terminated. It is also shown in figure 5a that the limited strain softening was observed in the $d\varepsilon_v/d\varepsilon_1 = -1$ path test. In this test, a material strain softening initially occurred and then the phase transformation state (PT) characterised by the minimum value of deviatoric stress was reached. After that a strain hardening behaviour was observed and eventually the banding strain softening occurred.

The excess pore water pressures developed in the tests are shown in figure 5b. It can be seen that the higher the strain increment ratio imposed, the more negative the pore water pressure change. It is noted that the excess pore water pressure developed in an undrained test is not the highest, as often assumed. The pore water generation for the undrained path is in between that for a negative (dilative) strain path and a positive (compressive) strain path.

The effective stress paths obtained from the strain paths tests are plotted in figure 5c. Except the test with $d\varepsilon_v/d\varepsilon_1 = -1.0$, all the other paths show a tendency to approach the asymptotic line. It can be observed that the higher (i.e., the more positive) the strain increment ratio, the lower the asymptotic stress ratio η_{asy}. This can also be

seen from the q/p' versus ε_1 curves shown in figure 5d. However, due to shear band formation, strain softening and thus a reduction in q/p' occurred in some tests (figures 5a and 5d). It is also observed that although η_{asy} increases with an increase in the dilatancy ratio ($-d\varepsilon_v/d\varepsilon_1$), the η_{asy} approached in the tests with $d\varepsilon_v/d\varepsilon_1 = -0.4$, -0.6, and -1.0 is about the same value of $\eta_{max} = 1.45$. Therefore, it appears to be a limiting value, η_{max}. When ($-d\varepsilon_v/d\varepsilon_1$) exceeds a certain value, η_{asy} will only reach this limiting value.

Strain path tests on very loose sand. The results of a series of strain path tests conducted on very loose sand with strain increment ratios $d\varepsilon_v/d\varepsilon_1$ ranging from +0.6 to –0.6 are presented in figure 6. The void ratios e_c of specimens after K_0 consolidation were in between 0.887 and 0.903, corresponding to relative densities Dr_c = 3–10%. All the specimens were prepared by the MT method. The effect of strain paths on the stress–strain behaviour of very loose sand can be seen in figure 6a, where the stress–strain curves are plotted. By imposing a more compressive (positive) strain increment ratio, a sand specimen shows a stiffer behaviour. Similarly, when the strain increment ratio becomes more negative (dilative) a specimen exhibits more pronounced strain softening. It is also observed that in an undrained condition ($d\varepsilon_v/d\varepsilon_1 = 0$) strain softening occurs for very loose sand. The curves representing excess pore water pressure versus axial strain for very loose sand are presented in figure 6b. The positive pore water pressure development was observed when $d\varepsilon_v/d\varepsilon_1 < 0$. Negative pore water pressure response was obtained when $d\varepsilon_v/d\varepsilon_1 > 0$. The more negative the $d\varepsilon_v/d\varepsilon_1$ imposed, the more positive the excess pore water pressure change.

The effective stress paths obtained from the tests on very loose sand are presented in figure 6c. The CSL line obtained from drained plane-strain tests on very loose sand is also plotted in figure 6c for comparison. The stress paths obtained from compressive strain paths exhibit strain-hardening behaviour, while the stress paths obtained from dilative strain paths exhibit strain-softening behaviour. Nevertheless, it can be seen from figure 6c that the stress paths resulting from tests with $d\varepsilon_v/d\varepsilon_1 < 0.2$ approached the CSL. The stress paths obtained from tests with $d\varepsilon_v/d\varepsilon_1 = +0.4$ and +0.6 approached the corresponding asymptotic lines. The $q/p'-\varepsilon_1$ curves are presented in figure 6d. It is seen that all the curves tend to approach asymptotically a constant value of q/p'. The limiting stress ratio η_{max} for loose sand appears to be $\eta_{cs} = 1.16$.

6. SHEAR BAND FORMATION

Shear band formation in drained and undrained plane-strain compression tests has been observed by a number of researchers [2], [11], [12], [13], [25]. However, the shear band formation in other than $d\varepsilon_v/d\varepsilon_1 = 0$ (undrained) strain paths has not been reported before.

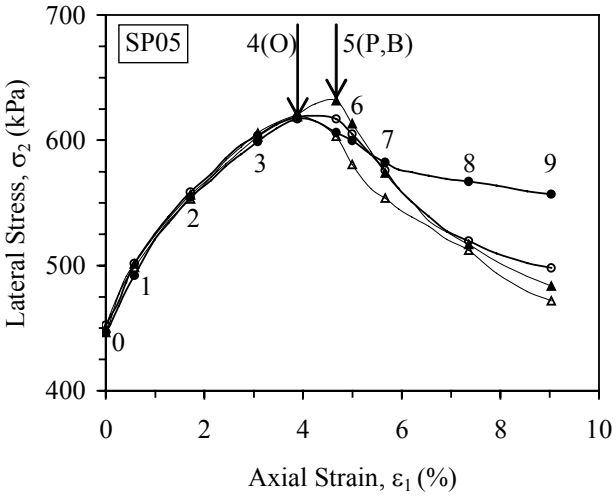
SP05
4(O)
5(P,B)
Lateral Stress, σ2 (kPa)
Axial Strain, ε1 (%)
700
600
500
400
0
2
4
6
8
10
0
1
2
3
6
7
8
9

a)

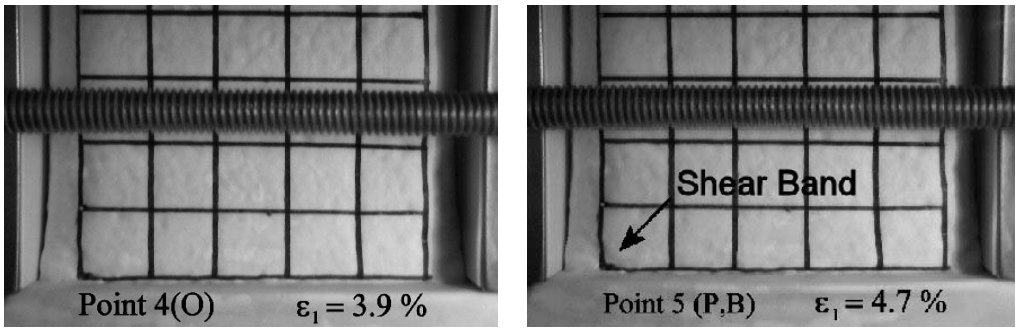
Point 4(O) ε1 = 3.9 %
Shear Band
Point 5 (P,B) ε1 = 4.7 %

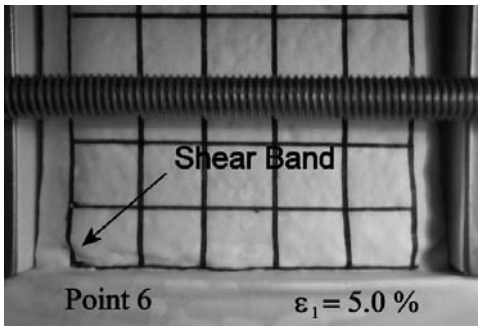
Shear Band
Point 6 ε1 = 5.0 %

b)

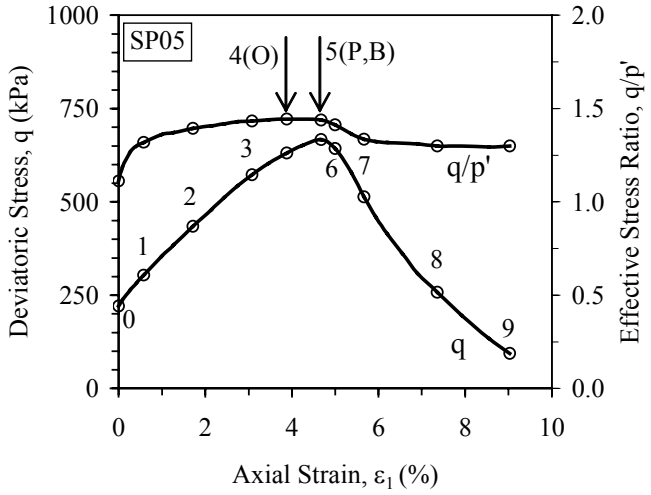

c)

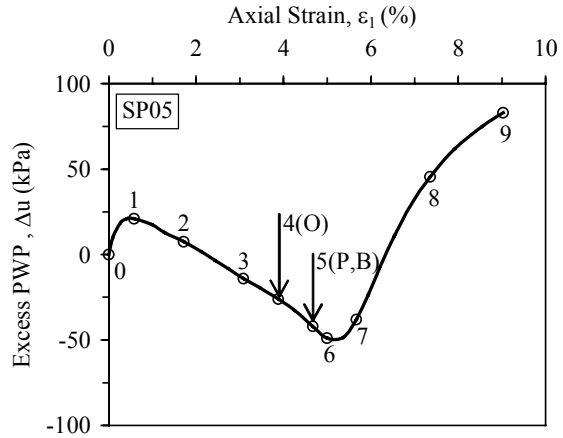

d)

Fig. 7. Shear band development in Test SP05:
a) σ_2 versus ε_1 curves, b) selected photographs, c) q versus ε_1 and q/p' versus ε_1 curves, d) Δu versus ε_1 curves

During all the plane-strain tests presented in this study, the process of shear band formation has been monitored by taking photographs at a close time interval using a high-resolution digital camera. Grid lines were marked on the membrane surface facing the camera (σ_3 plane) to facilitate the observation of the shear band. The occurrence of the shear bands was also detected by comparing the σ_2–ε_1 curves obtained

from the four individual pressure transducers. In this investigation, shear bands only occurred for medium loose to medium dense specimen with $d\varepsilon_v/d\varepsilon_1 \leq 0$ imposed. For all the other strain path tests, including those on very loose sand, shear bands were not detected.

The results of a strain path test SP05 conducted on a medium dense specimen (e_c = 0.677) using $d\varepsilon_v/d\varepsilon_1 = -0.4$ are presented in figure 7. The $\sigma_2-\varepsilon_1$ curves obtained from the four load cells during Test SP05 are presented in figure 7a. The numbers marked on the stress–strain curves shown in figure 7a refer to the points where photographs of the specimens were taken. Selected photographs taken around the shear band being formed are shown in figure 7b. For more details, see [39], [40]. It can be seen from figure 7a that at the point 4, the σ_2 values measured by each load cell start to diverge. However, from the photographs, the shear band became visible at the point 5, which was after the point 4. Therefore, the point 4, where σ_2 starts to diverge, can be used as an indicator for the onset of the shear band. As shown in figure 7c, the point 5, where the shear band became visible, is the peak point on the $q-\varepsilon_1$ curve. It can also be seen from figure 7d that the pore water pressure started to increase just after the point 5 which is another indication that shear band had occurred. The above results indicate that when the shear band occurs, the lateral stress distributions become highly non-uniform. Therefore, the point, where the σ_2 curves start to diverge, indicates the point where shear band has been initiated. The results obtained from plane-strain tests under strain path controlled conditions also show that the shear band develops in the specimen earlier than its physical appearance on the membrane surface.

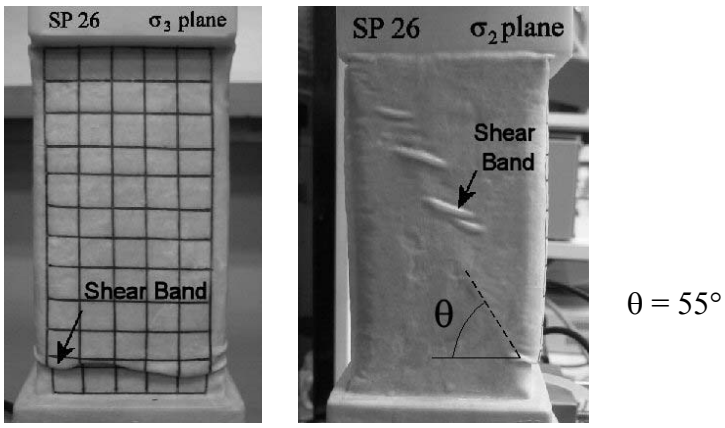

Fig. 8. A shear band observed at the end of Test SP26

The typical mode of the shear bands developed during strain path tests is identical to that obtained under drained and undrained conditions [39], [40]. An example of the shear band observed at the end of Test SP26 is shown in figure 8. The photographs

(figure 8) were taken after the cell was dismounted and a vacuum was applied to hold the sample. It can be seen that the specimen slides towards the σ_3 direction. Therefore, the shear band on the σ_3 plane is nearly horizontal and on the σ_2 plane is inclined at an angle $\theta = 55°$. The inclination θ for all the other shear bands measured in plane-strain tests was in the range of 49.0°–57.5° for medium loose sand and in the range of 49.6°–58.6° for medium dense sand. The average values of 55.6° and 56.2° were obtained for medium loose sand and medium dense sand, respectively. It has been observed that shear band inclinations were best predicted by the Roscoe solution [39], [40].

7. DISCUSSION

The experimental results presented in this paper clearly demonstrate that stress–strain behaviour of sand under plane-strain condition is strain path-dependent. The results show that the more positive strain increment ratio leads to the stiffer response of soil. Depending on the density, when a $d\varepsilon_v/d\varepsilon_1$ more negative than a certain value is imposed, strain softening will occur. This is consistent with the observations made for axisymmetric conditions based on triaxial test results [3], [7], [8], [19], [35], [36]. However, under plane-strain conditions shear bands would occur in medium loose and medium dense specimens. The occurrence of shear bands can lead to strain softening behaviour in post-peak region. Under axisymmetric conditions, shear bands would not occur, if free-ends were used to reduce end frictions. Therefore, the strain softening behaviour under plane-strain conditions as presented above is classified into two types. The first type is the material softening occurring for very loose sand as shown in figure 6 for tests with $d\varepsilon_v/d\varepsilon_1$ of 0.0 (undrained), –0.2, –0.4, and –0.6. This type of softening is the true element behaviour and it reflects the response of loose granular soils to the strain path imposed. The second type is the strain softening observed in hardening regime for medium loose and dense sand after the occurrence of shear band, for example, test $d\varepsilon_v/d\varepsilon_1 = 0.0$ (undrained), –0.2, –0.4, or –0.6 for medium dense sand in figure 5. This type of strain softening is caused by the formation of shear band in the hardening regime. This type of strain softening has been termed as *banding softening* by CHU et al. [9].

The asymptotic state of sand has been investigated by CHU and LO [8] under axisymmetric and three-dimensional stress conditions. It was found that the η_{asy} is independent of the soil stress history and the initial effective confining stress. CHU and LO [8] also concluded that there is a relationship between the controlled strain increment ratio $d\varepsilon_v/d\varepsilon_1$ and the asymptotic stress ratio η_{asy}. This relationship is independent of the initial effective confining stress, the loading mode and shearing rate and is not significantly affected by the void ratio.

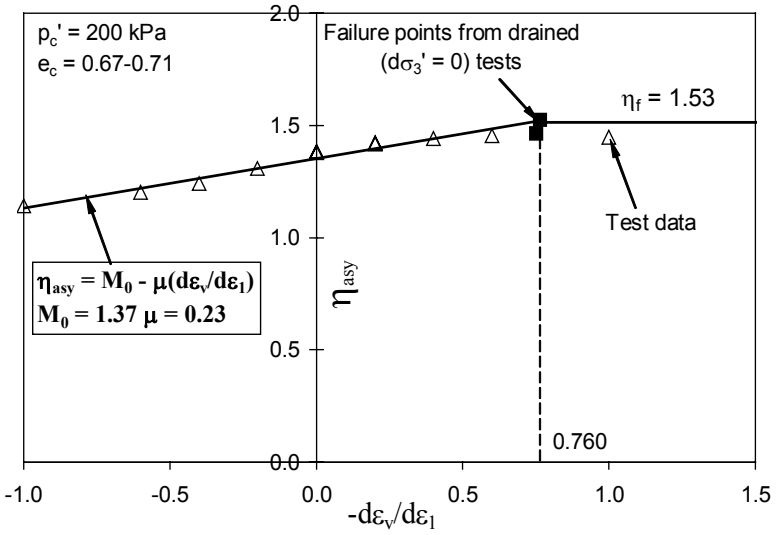

Fig. 9. Relationship between η_{asy} and $(-d\varepsilon_v/d\varepsilon_1)$

The experimental data obtained from the strain path tests conducted on medium dense sand (e_c = 0.67–0.71) and commenced with p'_c = 200 kPa under plane-strain conditions is presented in figure 9. Figure 9 shows that there is a relationship between η_{asy} and $d\varepsilon_v/d\varepsilon_1$ at the asymptotic state. By fitting the line through all the data points, the empirical equation between the asymptotic stress ratio and the strain increment ratio in strain path tests of $-0.6 \le d\varepsilon_v/d\varepsilon_1 \le 1$ can be established:

$$\eta_{asy} = M_0 - \mu\left(\frac{d\varepsilon_v}{d\varepsilon_1}\right), \tag{1}$$

where: M_0 = 1.37 and μ = 0.23 are the experimental constants. Similar relationship can be established for any density state [39].

Equation (1) shows that the asymptotic stress ratio increases with a decrease in the controlled strain increment ratio. However, as discussed earlier, the achievable stress ratio is bounded by a limiting value of η_{asy}. Furthermore, it has been established by CHU and LO [8] under axisymmetric conditions that the maximum achievable asymptotic stress ratio η_{max} is bounded by the failure line determined by drained tests. In other words, when the controlled strain increment ratio $(d\varepsilon_v/d\varepsilon_1)_i$ is more negative than the strain increment ratio at failure $(d\varepsilon_v/d\varepsilon_1)_f$, the asymptotic stress ratio can only reach its limit value, the failure stress ratio η_f.

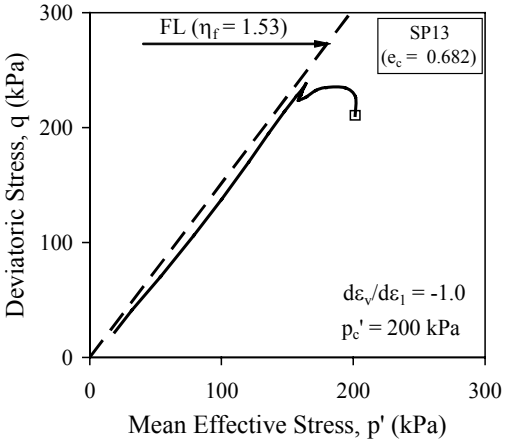

Fig. 10. Effective stress path of a $d\varepsilon_v/d\varepsilon_1 = -1.0$ test

The effective stress path resulting from a $d\varepsilon_v/d\varepsilon_1 = -1.0$ test is presented in figure 10. Fairly detailed results of this test have been given earlier in figure 5. Although the strain increment ratio imposed in the test is more negative than $(d\varepsilon_v/d\varepsilon_1)_f = -0.76$ determined for the same $p_c' = 200$ kPa (see figure 4e), the effective stress path approaches the failure line. Therefore, just as under the axisymmetric conditions, $(d\varepsilon_v/d\varepsilon_1)_f$ seems to be a threshold strain increment ratio under plane-strain conditions. When the controlled strain increment ratio is more negative than the strain increment ratio at failure, which in this case is –0.76, the asymptotic stress ratio can only reach its limit value, the failure stress ratio η_f. Thus, for the strain path tests with $d\varepsilon_v/d\varepsilon_1 < (d\varepsilon_v/d\varepsilon_1)_f$:

$$\eta_{\text{asy}} = \eta_f \,, \tag{2}$$

where η_f is the failure stress ratio.

Combining equations (1) and (2), the empirical relationship between the asymptotic stress ratio and a constant strain increment ratio can be established:

$$\eta_{\text{asy}} = \begin{cases} M_0 - \mu \dfrac{d\varepsilon_v}{d\varepsilon_1} & \text{for} \quad \dfrac{d\varepsilon_v}{d\varepsilon_1} \geq \left(\dfrac{d\varepsilon_v}{d\varepsilon_1}\right)_f, \\ \eta_f & \text{for} \quad \dfrac{d\varepsilon_v}{d\varepsilon_1} < \left(\dfrac{d\varepsilon_v}{d\varepsilon_1}\right)_f. \end{cases} \tag{3}$$

For the data shown in figure 9, $M_0 = 1.37$, $\mu = 0.23$, and $\eta_f = 1.53$. This relationship is consistent with that obtained under axisymmetric conditions [8].

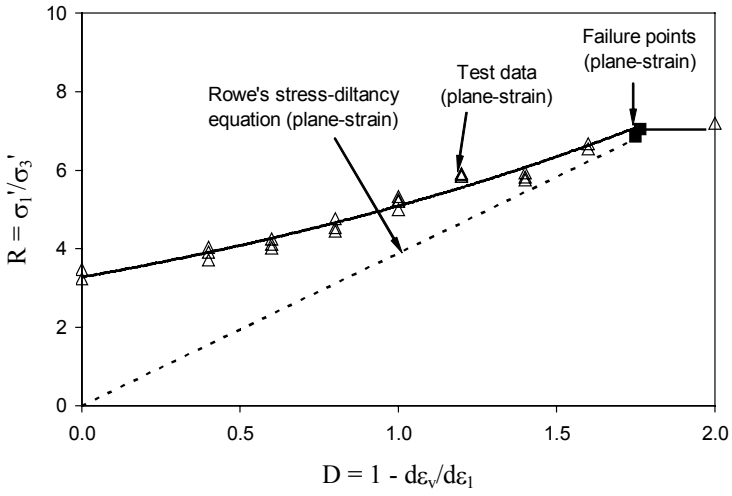

Fig. 11. Stress ratio versus dilatancy plot in plane-strain

In figure 11, the data obtained from the strain path tests is compared with Rowe's stress–dilatancy equation [29] for drained tests, expressed by:

$$\frac{\sigma_1'}{\sigma_3'} = K\left(1 - \frac{d\varepsilon_v}{d\varepsilon_1}\right), \tag{4}$$

where K is an experimental constant related to the friction angle at the critical state. For the Changi sand tested under plane-strain conditions, K = 3.85 [39]. The failure points obtained from drained tests are also plotted in figure 11. It should be mentioned that in Rowe's stress–dilatancy theory, the stress–dilatancy behaviour is assumed to be independent of the initial effective confining stress. However, as is shown in figure 4e, this assumption is not valid for the Changi sand tested under plane-strain conditions. Since all the strain path tests presented in figure 11 were commenced with the initial effective confining stress of 200 kPa, only the failure points obtained for the same p_c' were plotted in this figure. By comparing the curve obtained experimentally with that obtained from Rowe's stress–dilatancy theory, it can be seen that the stress ratio achieved in a constant strain increment ratio path test is higher than that in a drained test for the same dilatancy. Thus, it is clear that equation (4) cannot predict the asymptotic response in a strain path test under plane-strain conditions. The two curves only merge with one another at the failure state, which proves that the stress ratio at failure is independent of the stress–strain path leading to the failure. A horizontal line drawn to the right-hand side of the failure points in figure 11 represents the limit surface expressed by equation (2).

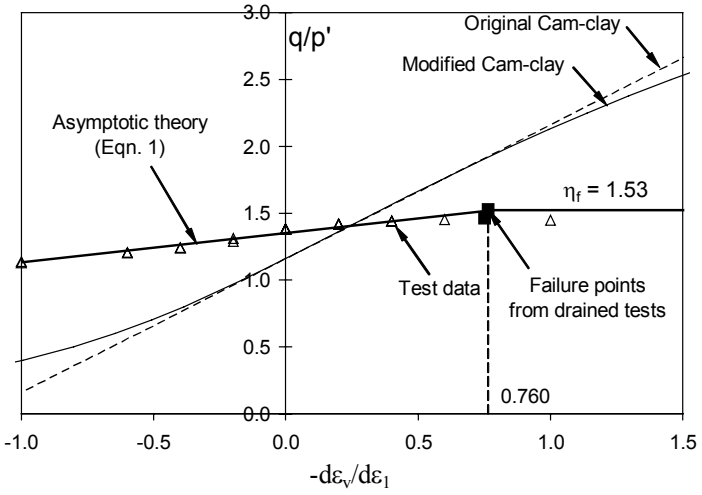

Fig. 12. Comparison of stress–dilatancy plots obtained from asymptotic theory and Cam clay models for plane-strain conditions

The data obtained from the strain path tests under plane-strain conditions is also compared with the original Cam clay model [27] and the modified Cam clay model [28], as shown in figure 12. In the original Cam clay model, the stress–dilatancy relation is defined by

$$\eta = \eta_{cs} - \frac{d\varepsilon_v}{d\varepsilon_s}, \tag{5}$$

where η_{cs} is the stress ratio at the critical state, as determined by drained tests (η_{cs} = 1.16 in this paper). The modified Cam clay equation is expressed by:

$$\frac{d\varepsilon_v}{d\varepsilon_s} = \frac{\eta_{cs}^2 - \eta^2}{2\eta}. \tag{6}$$

It can be seen from figure 12 that equations (5) and (6) cannot predict the asymptotic behaviour of sand in a strain path test under plane-strain conditions. This is consistent with the observations made under axisymmetric conditions [3], [8].

8. CONCLUSIONS

In this paper, the asymptotic behaviour of a granular soil under plane-strain conditions was studied. The results can be summarized as follows:

- In a strain path test, both pore water pressure and volumetric strain are being changed. Therefore, strain path tests can be used to simulate various drainage condi-

tions. The stress–strain behaviour of soil under strain path-controlled conditions is not bounded by undrained ($d\varepsilon_v/d\varepsilon_1 = 0$) and drained behaviour.

• The stress–strain behaviour of sand under plane-strain conditions is strain path-dependent. When the strain increment ratio $(d\varepsilon_v/d\varepsilon_1)_i$ imposed on the specimen is higher (i.e., more positive) than a threshold value, strain hardening behaviour will prevail. On the other hand, when $(d\varepsilon_v/d\varepsilon_1)_i$ is lower (i.e., more negative) than a threshold value, strain softening will occur. The threshold strain increment ratio is defined by $(d\varepsilon_v/d\varepsilon_1)_f$, that is the strain increment ratio at failure as measured in a drained test. This is consistent with the observations made for axisymmetric conditions based on triaxial test results [3], [6], [7], [8], [19], [35].

• When medium dense sand is sheared under $d\varepsilon_v/d\varepsilon_1 = \text{const}$ path, the resulting effective stress path will approach asymptotically a constant stress ratio line (CSRL). The lower (i.e., more negative) the imposed strain increment ratio, the higher the resultant asymptotic stress ratio, η_{asy}. The relationship between the imposed strain increment ratio and the resultant constant stress ratio can be experimentally determined. For plane-strain conditions, the relationship can be expressed by:

$$\eta_{\text{asy}} = \begin{cases} M_0 - \mu \dfrac{d\varepsilon_v}{d\varepsilon_1} & \text{for} \quad \dfrac{d\varepsilon_v}{d\varepsilon_1} \geq \left(\dfrac{d\varepsilon_v}{d\varepsilon_1}\right)_f, \\ \eta_f & \text{for} \quad \dfrac{d\varepsilon_v}{d\varepsilon_1} < \left(\dfrac{d\varepsilon_v}{d\varepsilon_1}\right)_f, \end{cases}$$

where $M_0 = 1.37$ and $\mu = 0.23$ are the experimental constants obtained from plane-strain tests. This relationship is consistent with that obtained under axisymmetric conditions by CHU and LO [8].

• The asymptotic behaviour of sand cannot be successfully predicted by the Cam clay models nor cannot be predicted by the Rowe's stress–dilatancy equation.

ACKNOWLEDGEMENTS

The experimental data presented in this paper has been obtained during the author's doctoral study in Singapore. The research scholarship provided by Nanyang Technological University is gratefully acknowledged. The author also wishes to thank British Council for the financial support of his Visiting Fellowship at UNSW@ADFA in Canberra.

REFERENCES

[1] ADALIER K., ELGAMAL A.-W., *Seismic response of adjacent dense and loose saturated sand columns*, Soil Dynamics and Earthquake Engineering, 2002, Vol. 22, 115–127.

[2] ALSHIBLI A.K., BATISTE S.N., STURE S., *Strain localization in sand: plane strain versus triaxial compression*, Journal of Geotechnical and Geoenvironmental Engineering, 2003, Vol. 129, No. 6, 483–494.

[3] ASAKA Y., TOKIMATSU K., IWASAKI K., SHAMOTO Y., *A simple stress–strain relation based on stress-path behaviour in strain-path controlled triaxial tests*, Soils and Foundations, 2003, Vol. 43, No. 2, 33–68.

[4] CASTRO G., *Liquefaction of sands*, Harvard Soil Mechanics Series, 1969, No. 81, 1–112.

[5] CHU J., LO S.-C.R., *On the implementation of strain path testing*, Proceedings of the 10th European Conference on Soils Mechanics and Foundations Engineering, Florence, Italy, 1991, Vol. 1, 53–56.

[6] CHU J., LO S.-C.R., LEE I.K., *Strain softening behavior of a granular soil in strain path testing*, Journal of Geotechnical Engineering, 1992, Vol. 118, No. 2, 191–208.

[7] CHU J., LO S.-C.R., LEE, I.K., *Instability of granular soils under strain path testing*, Journal of Geotechnical Engineering, 1993, Vol. 119, No. 5, 874–892.

[8] CHU J., LO S.-C.R., *Asymptotic behaviour of a granular soil in strain path testing*, Géotechnique, 1994, Vol. 44, No. 1, 65–82.

[9] CHU J., LO S.-C.R., LEE I.K., *Strain softening and shear band formation of sand in multi-axial testing*, Géotechnique, 1996, Vol. 46, No. 1, 63–82.

[10] CHU J., LEONG W.K., *Pre-failure strain softening and pre-failure instability of sand: a comparative study*, Géotechnique, 2001, Vol. 51, No. 4, 311–321.

[11] DESRUES J., VIGGIANI G., *Strain localization in sand: an overview of the experimental results obtained in Grenoble using stereophotogrammetry*, International Journal for Numerical and Analytical Methods in Geomechanics, 2004, Vol. 28, No. 4, 279–321.

[12] FINNO R.J., HARRIS W.W., VIGGIANI G., *Strain localization and undrained steady state of sand*, Journal of Geotechnical Engineering, 1996, Vol. 122, No. 6, 462–473.

[13] FINNO R.J., HARRIS W.W., MOONEY M.A., VIGGIANI G., *Shear bands in plane strain compression of loose sand*, Géotechnique, 1997, Vol. 47, No. 1, 149–165.

[14] GUDEHUS G., GOLDSCHEIDER M., WINTER H., *Mechanical properties of sand and clay and numerical integration methods: some sources of errors and bounds of accuracy*, Finite Elements in Geomechanics, Gudehus G. (Ed.), 1977, 121–150.

[15] LADE P.V., DUNCAN J.M., *Stress-path dependent behaviour of cohesionless soil*, Journal of Geotechnical Engineering Division, 1976, Vol. 102, No. GT1, 51–68.

[16] LADE P.V., NELSON R.B., ITO Y.M., *Instability of granular materials with nonassociated flow*, Journal of Engineering Mechanics, 1988, Vol. 114, No. 12, 2173–2191.

[17] LADE P.V., *Static instability and liquefaction of loose fine sandy slopes*, Journal of Geotechnical Engineering, 1992, Vol. 118, No. 1, 51–71.

[18] LAMBE T.W., *Stress path method*, Journal of Soil Mechanics and Foundation Division, 1967, Vol. 93, No. SM6, 309–331.

[19] LANCELOT L., SHAHROUR I., AL MAHMOUD M., *Instability and static liquefaction on proportional strain paths for sand at low stresses*, Journal of Engineering Mechanics, 2004, Vol. 130, No. 11, 1365–1372.

[20] LEONG W.K., CHU J., TEH C.I., *Liquefaction and instability of a granular fill material*, Geotechnical Testing Journal, 2000, Vol. 23, No. 2, 178–192.

[21] LO S.-C.R., CHU J., LEE I.K., *A technique for reducing membrane penetration and bedding errors*, Geotechnical Testing Journal, 1989, Vol. 12, No. 4, 311–316.

[22] LO S.-C.R., LEE I.K., *Response of granular soil along constant stress increment ratio path*, Journal of Geotechnical Engineering, 1990, Vol. 116, No. 3, 355–376.

[23] LO S.-C.R., CHU J., *The measurement of K_0 by triaxial strain path testing*, Soils and Foundations, 1991, Vol. 31, No. 2, 181–187.

[24] MENZIES B.K., *A computer controlled hydraulic triaxial testing system*, Advanced Triaxial Testing of Soil and Rock, ASTM STP 977, R.T. Donaghe, R.C. Chaney, and M.L. Silver (Eds.), 1988, ASTM, Philadelphia, 82–94.
[25] MOKNI M., DESRUES J., *Strain localisation measurements in undrained plane-strain biaxial tests on Hostun RF sand*, Mechanics of Cohesive-Frictional Materials, 1988, Vol. 4, 419–441.
[26] National Research Council (NRC), *Liquefaction of soils during earthquakes*, Committee on Earthquake Engineering, Commission on Earthquake and Technical Systems, National Academies Press, 1985, Washington, D.C.
[27] ROSCOE K.H., SCHOFIELD A.N., *Mechanical behaviour of an idealised 'wet' clay*, [in:] Proceedings of the 1st European Conference on Soil Mechanics and Foundation Engineering, Wiesbaden, Germany, 1963, Vol. 1, 47–54.
[28] ROSCOE K.H., BURLAND J.B., *On the generalized stress–strain behaviour of 'wet' clay*, Engineering Plasticity, J. Heyman and F.A. Leckie (Eds.), Cambridge University Press, New York, 1968, 535–609.
[29] ROWE P.W., *The stress–dilatancy relationship for static equilibrium of an assembly of particles in contact*, Proceedings of Royal Society, 1962, Vol. A269, 500–527.
[30] ROWE P.W., BARDEN L., *Importance of free ends in triaxial testing*, Journal of Soil Mechanics and Foundation Division, 1964, Vol. 90, No. SM1, 1–15.
[31] SHAMOTO Y., ZHANG J.-M., KASUKAME T., *A simple method for triaxial strain path testing*, Soils and Foundations, 1996, Vol. 36, No. 2, 129–137.
[32] SKEMPTON A.W., *Standard penetration test procedures and effects in sand of overburden pressure, relative density, particle size, ageing, and overconsolidation*, Géotechnique, 1986, Vol. 36, No. 3, 425–447.
[33] SLADEN J.A., D'HOLLANDER R.D., KRAHN J., *The liquefaction of sands, a collapse surface approach*, Canadian Geotechnical Journal, 1985, Vol. 22, No. 4, 564–578.
[34] TOPOLNICKI M., GUDEHUS G., MAZURKIEWICZ B.K., *Observed stress–strain behaviour of remoulded saturated clay under plane-strain conditions*, Géotechnique, 1990, Vol. 42, No. 2, 155–187.
[35] VAID Y.P., ELIADORANI A., *Instability and liquefaction of granular soils under undrained and partially drained states*, Canadian Geotechnical Journal, 1998, Vol. 35, No. 6, 1053–1062.
[36] VAID Y.P., ELIADORANI A., *Undrained and drained(?) stress–strain response*, Canadian Geotechnical Journal, 2000, Vol. 37, No. 5, 1126–1130.
[37] VAID Y.P., SIVATHAYALAN S., *Fundamental factors affecting liquefaction susceptibility of sands*, Canadian Geotechnical Journal, 2000, Vol. 37, No. 3, 592–606.
[38] VAID Y.P., ELIADORANI A., SIVATHAYALAN S., UTHAYAKUMAR M., *Laboratory characterization of stress–strain behavior of soils by stress and/or strain path loading*, Geotechnical Testing Journal, 2001, Vol. 24, No. 2, 200–208.
[39] WANATOWSKI D., *Strain softening and instability of sand under plane-strain conditions*, Ph.D. thesis, Nanyang Technological University, Singapore, 2005.
[40] WANATOWSKI D., CHU J., *Stress–strain behaviour of a granular fill measured by a new plane-strain apparatus*, Geotechnical Testing Journal, 2006, Vol. 29, No. 2, 149–157.
[41] WANATOWSKI D., CHU J., *Static liquefaction of sand in plane-strain*, Canadian Geotechnical Journal, 2007, Vol. 44, No. 3, 299–313.